Intercalating Polycyclic Aromatic Hydrocarbon−DNA Adducts Poison DNA Religation by Vaccinia Topoisomerase and Act as Roadblocks to Digestion by Exonuclease III†

Lyudmila Yakovleva,‡ Christopher J. Handy,§ Haruhiko Yagi,§ Jane M. Sayer,§ Donald M. Jerina,§ and Stewart Shuman*,‡

Molecular Biology Program, Sloan-Kettering Institute, New York, New York 10021, and Laboratory of Bioorganic Chemistry, NIDDK, National Institutes of Health, Bethesda, Maryland 20892

Received January 24, 2006; Revised Manuscript Received April 16, 2006

ABSTRACT: Polycyclic aromatic hydrocarbon (PAH)−DNA adducts pervert the execution or fidelity of enzymatic DNA transactions and cause mutations and cancer. Here, we examine the effects of intercalating PAH−DNA adducts on the religation reaction of vaccinia DNA topoisomerase, a prototypal type IB topoisomerase (TopIB), and the 3′ end-resection reaction of *Escherichia coli* exonuclease III (ExoIII), a DNA repair enzyme. Vaccinia TopIB forms a covalent DNA-(3′-phosphotyrosyl)-enzyme intermediate at a target site 5′-$C^{+5}C^{+4}C^{+3}T^{+2}T^{+1}p\downarrow N^{-1}$ in duplex DNA. The rate of the forward cleavage reaction is suppressed to varying degrees by benzo[*a*]pyrene (BP) or benzo[*c*]phenanthrene (BPh) adducts at purine bases within the 3′-$G^{+5}G^{+4}G^{+3}A^{+2}A^{+1}T^{-1}A^{-2}$ sequence of the nonscissile strand. We report that BP adducts at the +1 and −2 N^6-deoxyadenosine (dA) positions flanking the scissile phosphodiester slow the rate of DNA religation to a greater degree than they do the cleavage rate. By increasing the cleavage equilibrium constant ≥10-fold, the BPdA adducts, which are intercalated via the major groove, act as TopIB poisons. With respect to ExoIII, we find that (i) single BPdA adducts act as durable roadblocks to ExoIII digestion, which is halted at sites 1 and 2 nucleotides prior to the modified base; (ii) single BPhdA adducts, which also intercalate via the major groove, elicit a transient pause prior to the lesion, which is eventually resected; and (iii) BPh adducts at N^2-deoxyguanosine, which intercalate via the minor groove, are durable impediments to ExoIII digestion. These results highlight the sensitivity of repair outcomes to the structure of the PAH ring system and whether intercalation occurs via the major or minor groove.

Polycyclic aromatic hydrocarbons (PAHs[1]) such as benzo[*a*]pyrene (BP) and benzo[*c*]phenanthrene (BPh) are potent environmental carcinogens. BP and BPh are converted in vivo to bay- or fjord-region diol epoxides (*1*), which react with the deoxyadenosine (dA) or deoxyguanosine (dG) bases in DNA to form covalent PAH−DNA adducts (*2*). Recent studies of PAH−DNA adducts have focused on elucidating their molecular structures (reviewed in ref 3 (*3*)) and their impact on individual enzymes involved in DNA replication and repair. PAH−DNA adducts can either reside within the DNA minor groove (e.g., a BPdG adduct derived from the trans opening of the BP diol epoxide) or intercalate between the base pairs flanking the lesion (e.g., BPdA, BPhdA, and BPhdG adducts; for examples of adduct structures see Figures 1A and 6A). The orientation of the trans BPdG adduct in the minor groove and the direction of intercalation of the BPdA, BPhdA and BPhdG adducts (either 5′ or 3′ of the modified base) is dictated by the absolute stereochemical configuration at the point of attachment of the exocyclic amino group of the purine base to the diol epoxide. The ability to synthesize oligodeoxynucleotides containing single PAH adducts of defined chirality has spurred studies of their impact on DNA polymerases (*4*−*6*) and DNA topoisomerases (*7*−*10*) as potential mediators of PAH-induced mutations.

Type IB DNA topoisomerase (TopIB) modulates DNA supercoiling by cleaving and rejoining one strand of the DNA duplex through a transient DNA-(3′-phosphotyrosyl)-enzyme intermediate. Human TopIB is the target of the camptothecin anticancer drugs (*11*), which are classified as TopIB poisons because they exert their cytotoxicity by selectively impeding the TopIB religation reaction, which leads to the accumulation of nicked covalent TopIB−DNA adducts that give rise during replication to lethal double-strand breaks. Many natural DNA lesions, including PAH−DNA adducts (*7*−*9*), are also capable of skewing the cleavage−religation equilibrium of human TopIB. Two classes of PAH effects on

† This work was supported by NIH Grant GM46330 (S.S.) and the Intramural Research Program of the National Institute of Diabetes, Digestive and Kidney Diseases (D.M.J.).

* Corresponding author. Tel: (212) 639-7145. Fax: (212) 717-3623. E-mail: s-shuman@ski.mskcc.org.

‡ Sloan-Kettering Institute.

§ National Institutes of Health.

[1] Abbreviations: PAH, polycyclic aromatic hydrocarbon; BP, benzo[*a*]pyrene; BPh, benzo[*c*]phenanthrene; TopIB, type IB DNA topoisomerase; ExoIII, *Escherichia coli* exonuclease III; BPdA, BPhdA, adducts derived from the ring opening of BP and BPh diol epoxides, respectively, by the exocyclic 6-amino group of deoxyadenosine; BPdG, BPhdG, adducts derived from the ring opening of BP and BPh diol epoxides, respectively, by the exocyclic 2-amino group of deoxyguanosine.

10.1021/bi060158h CCC: $33.50
Published on Web 05/26/2006

human TopIB have been described, whereby an adduct either (i) suppresses cleavage at the normal recognition site on the scissile strand but promotes alternative cleavages elsewhere on the DNA substrate or (ii) enhances the extent of equilibrium cleavage at the normal site by poisoning the religation step.

Studies of the effects of PAH−DNA adducts on vaccinia virus TopIB have complemented and extended the initial findings made with the human enzyme (*12*−*14*). Vaccinia TopIB is distinguished from its human counterpart by its stringent site specificity in DNA transesterification (*15*). Vaccinia TopIB binds and cleaves duplex DNA at a pentapyrimidine target sequence 5′-$C^{+5}C^{+4}C^{+3}T^{+2}T^{+1}p\downarrow N^{-1}$. The Tp↓ nucleotide (defined as the +1 nucleotide) becomes linked to Tyr274 of the topoisomerase. Vaccinia TopIB is especially amenable to quantitative DNA modification interference studies because the pre-steady-state kinetic parameters for transesterification are known (*16*−*18*) and, unlike human TopIB, the viral enzyme does not relinquish its site specificity in response to a DNA lesion. The interface of TopIB with the DNA minor groove was investigated by introducing BPdG adducts within the nonscissile 3′-$G^{+5}G^{+4}G^{+3}A^{+2}A^{+1}N^{-1}N^{-2}$ strand of a suicide cleavage substrate (*12*). A sharp margin of interference effects was observed, whereby +5 and −2 BPdG modifications were well tolerated, but +4, +3, and −1 BPdG adducts were severely deleterious. Stereoselective effects at the −1 nucleoside (the *R* diastereomer interfered, whereas the *S* diastereomer did not) delineated at high resolution the downstream border of the minor groove interface. The effects of intercalating PAH−DNA adducts on vaccinia TopIB were analyzed by placing BPh at all of the purines (and BP at all dA positions) of the 3′-$G^{+5}G^{+4}G^{+3}A^{+2}A^{+1}T^{-1}A^{-2}$ sequence of the nonscissile strand (*13*, *14*). We found that cleavage was suppressed by PAH intercalation between the +4/+3, +3/+2, +2/+1, +1/−1, and −1/−2 base pairs, but intercalation at the +6/+5, +5/+4, and −2/−3 base pairs had little effect. These findings finely demarcated the upstream and downstream margins of the interface between DNA and vaccinia TopIB.

Initial studies were limited to the analysis of the effects of the PAH adduct on the rate and extent of the forward transesterification reaction of vaccinia TopIB on a suicide cleavage substrate composed of a 34-mer scissile strand annealed to a series of 18-mer nonscissile strands containing a single PAH-purine adduct. Here we analyzed the effects of intercalating BP adducts on the kinetics of religation and the cleavage−religation equilibrium, which required new syntheses of 30-mer nonscissile strands containing chirally pure BPdA adducts at the +1A and −2A positions. We report that BPdA is a poison of vaccinia TopIB.

We also examined the effects of intercalating PAH−DNA adducts on the exonucleolytic resection reaction of the DNA repair enzyme *Escherichia coli* exonuclease III (ExoIII). It is thought that PAH−DNA adducts are especially mutagenic because they are refractory to elimination via DNA repair mechanisms (*19*−*21*). ExoIII possesses 3′-5′ exonuclease and abasic endonuclease activities and provides a structurally and biochemically defined paradigm for related nuclease activities in mammalian systems (*22*−*24*). In its exonuclease mode, ExoIII digests duplex DNA from the 3′ end to liberate 5′-dNMP products. Previously, we showed that DNAs containing BPdG adducts were protected from digestion by ExoIII, which was consistently arrested at positions 2 to 4-nt prior to the BP-modified guanosine (*12*). These results showed that ExoIII surveys the minor groove ahead of the active site of catalysis and that space-filling lesions in the minor groove strongly impede its progress. Here, we find that intercalating BPh and BP adducts also act as roadblocks to ExoIII but differ in their longevity of inhibition. Whereas single BPdA and BPhdG adducts are durable impediments to ExoIII digestion, single BPhdA adducts elicit a transient pause and are eventually excised.

EXPERIMENTAL PROCEDURES

Modified DNA Oligonucleotides. The 30-mers containing trans opened C-10 *S*- and *R*-BPdA adducts were synthesized using the pure C-10 *R* and C-10 *S* diastereomers (*10*) of the BPdA 5′-*O*-dimethoxytrityl-3′-cyanoethylphosphoramidites. Manual coupling of the modified phosphoramidites was performed as described for the synthesis of dG adducted oligonucleotides (*25*). The *S*- and *R*-BPdA-adducted oligonucleotides were purified by reverse phase HPLC. Initial purification exploited a Hamilton PRP-1 column (10 × 250 mm, 7 μm), which was eluted at 3.0 mL/min with a linear gradient that increased the percentage of solvent B in solvent A from 0 to 35% over 20 min at 25 °C (where solvent A is 0.1 M $(NH_4)_2CO_3$ at pH 7.5, and solvent B is a 1:1 mixture of A with acetonitrile at pH 7.5). The retention times ranged from 16.4 to 18.2 min. Further purification was performed with a Waters Xterra MS C_{18} column (4.6 × 50 mm, 2.5 μm), which was eluted at 1.0 mL/min with the same solvent gradient at 45 °C. The retention times ranged from 11.9 to 12.4 min. The oligonucleotide 18-mers containing *S* and *R* BP and BPh diol epoxide adducts were described previously (*13*, *14*).

DNA Substrates. The CCCTT-containing scissile strands were 5′-^{32}P-labeled by enzymatic phosphorylation in the presence of [γ-^{32}P]ATP and T4 polynucleotide kinase. The labeled oligonucleotides were gel-purified and hybridized to standard or modified nonscissile strand oligonucleotides at a 1:4 molar ratio of scissile to nonscissile strand. Annealing reaction mixtures containing 0.2 M NaCl and oligonucleotides as specified were heated to 80 °C and then slow-cooled to 22 °C. The hybridized DNAs were stored at 4 °C. The structures of the annealed duplexes and the sequences of the component strands are depicted in the Figures.

Single-Turnover DNA Cleavage. Reaction mixtures containing (per 20 μL) 50 mM Tris-HCl (pH 7.5), 0.3 pmol of CCCTT-containing DNA and 75, 150, or 300 ng (2, 4, or 8 pmol) of vaccinia TopIB were incubated at 37 °C. The reactions were initiated by adding TopIB to prewarmed reaction mixtures. Aliquots (20 μL) were withdrawn at the times specified and quenched immediately with SDS (1% final concentration). The products were analyzed by electrophoresis through a 10% polyacrylamide gel containing 0.1% SDS. The free DNA migrated near the dye front. Covalent complex formation was revealed by the transfer of radiolabeled DNA to TopIB. The extent of covalent complex formation was quantified by scanning the dried gel using a Fujifilm BAS2500 imager. A plot of the percentage of input DNA cleaved versus time established the endpoint values for cleavage. The data were then normalized to the

endpoint values (defined as 100%), and the cleavage rate constants (k_{cl}) were calculated by fitting the normalized data to the equation $100 - \%\text{cleavage}_{(\text{norm})} = 100e^{-kt}$.

Single-Turnover Religation by the Suicide Intermediate. Cleavage reaction mixtures containing (per 20 μL) 0.3 pmol of the 18-mer/30-mer DNA and 150 ng of TopIB were incubated at 37 °C for either 30 min (−2*R* and −2*S* BPdA substrates) or 120 min (+1*R* and +1*S* BPdA substrates) to form the suicide intermediate. Religation was initiated by the simultaneous addition of NaCl to 0.5 M concentration and a 5′-OH 18-mer acceptor strand d(ATTCCGATAGTGACTACA) to a concentration of 15 pmol/22 μL (a 50-fold molar excess over the input DNA substrate). Aliquots (22 μL) were withdrawn at the times specified in the Figures and adjusted immediately to 1% SDS. A time zero sample was withdrawn prior to the addition of the acceptor strand. The samples were digested for 60 min at 37 °C with 10 μg of proteinase K, then mixed with an equal volume of 95% formamide/20 mM EDTA, heat-denatured, and analyzed by electrophoresis through a 17% polyacrylamide gel containing 7 M urea in TBE (90 mM Tris-borate, 2.5 mM EDTA). The religation of the covalently bound 12-mer strand to the 18-mer acceptor DNA will yield a 5′-^{32}P-labeled 30-mer strand transfer product. The extent of religation (expressed as the percent of the covalent intermediate converted into the 30-mer) was plotted as a function of reaction time. The data were normalized to the endpoint values, and the religation rate constants (k_{rel}) were determined by fitting the data to the equation $(100 - \%\text{Rel}_{\text{norm}}) = 100e^{-kt}$.

Equilibrium Cleavage. A 34-mer CCCTT-containing oligonucleotide was 5′-^{32}P-labeled, then gel-purified, and annealed to an unlabeled complementary 30-mer strand to form a duplex containing 12 bp of DNA 5′ to the cleavage site and 18 bp 3′ to the cleavage site. The reaction mixtures containing (per 20 μL) 50 mM Tris-HCl (pH 7.5), 0.3 pmol of ^{32}P-labeled 34-mer/30-mer DNA, and 18, 37, 75, 150, or 300 ng of TopIB were incubated at 37 °C for either 30 min (−2*R* and −2*S* BPdA substrates) or 120 min (+1*R* and +1*S* BPdA substrates). The reactions were quenched by adding SDS to 1%. The samples were digested for 60 min at 37 °C with 10 μg of proteinase K, mixed with an equal volume of formamide/EDTA, and then analyzed by electrophoresis through a 17% polyacrylamide gel containing 7 M urea in TBE. The cleavage product, a ^{32}P-labeled 12-mer bound to a short peptide, was well resolved from the input 34-mer substrate. The extent of strand cleavage was quantified by scanning the gel. The cleavage equilibrium constant (K_{cl}) is defined as the ratio of covalently bound DNA to noncovalently bound DNA at the reaction endpoint under conditions of saturating enzyme and was calculated according to the equation $K_{cl} = \%\text{Cleaved}/(100 - \%\text{Cleaved})$.

Single-Turnover Religation on the 34-mer/30-mer DNA. Equilibrium cleavage reaction mixtures containing (per 20 μL) 0.3 pmol of ^{32}P-labeled 34-mer/30-mer DNA and 150 ng of TopIB were incubated at 37 °C to attain equilibrium. At this time (time zero), an aliquot (20 μL) was removed and quenched with SDS. The remainder of each reaction mixture was then adjusted to 0.5 M NaCl, and aliquots (21 μL) were taken at various times thereafter. The samples were digested with proteinase K and processed for electrophoresis as described in the preceding section. The decrease in the abundance of the covalent complex (expressed as percent of input DNA) was plotted as a function of time. The data were normalized to time zero and endpoint values, and k_{rel} was determined by fitting the data to the equation $\%\text{Cl}_{\text{norm}} = 100e^{-kt}$.

Exonuclease III Digestion. The 5′-^{32}P-labeled unmodified or PAH-adducted 18-mer oligonucleotides were hybridized to a complementary 34-mer DNA oligonucleotide at a 1:4 molar ratio of 18-mer to 34-mer. The reaction mixtures (60 μL) containing 66 mM Tris-HCl (pH 8.0), 0.66 mM $MgCl_2$, 1.8 pmol of labeled DNA, and 1 unit of *E. coli* ExoIII (New England Biolabs) were incubated at 22 °C. Aliquots (10 μL) were withdrawn at the times specified and quenched by adding EDTA to 30 mM final concentration. The samples were adjusted to 47% formamide, heat-denatured and analyzed by electrophoresis through a 17% denaturing polyacrylamide gel containing 7 M urea in TBE. The reaction products were visualized by an autoradiographic exposure of the gel.

RESULTS

BPdA Interference with DNA Religation by Vaccinia TopIB. The chemical structures of the C-10 *S* and *R* trans opened 7,8-diol 9,10-epoxide adducts of BP at the exocyclic N^6-amino group of deoxyadenosine (dA) are shown in Figure 1A. When present in duplex DNA, the *R* and *S* BPdA adducts intercalate from the major groove on the 5′ and 3′ sides of the modified base, respectively (Figure 1B), and perturb local base stacking (*26*−*30*). We previously used 34-mer/18-mer substrates composed of a 34-mer scissile strand and an adduct-containing 18-mer nonscissile strand to show that *R* and *S* BPdA modifications at +1A of the nonscissile strand sequence $3'\text{-G}^{+5}\text{G}^{+4}\text{G}^{+3}\text{A}^{+2}\text{A}^{+1}\text{T}^{-1}\text{A}^{-2}$ severely depressed the rate of single-turnover DNA cleavage by vaccinia TopIB, without affecting the yield of the covalent TopIB−DNA complex (*13*). In contrast, BPdA adducts at the −2 position had relatively little effect on the rate and extent of cleavage (*13*). The PAH adduct effects on the religation step were not examined initially because the 6-nucleotide 5′ overhang of the 12-mer-TopIB/18-mer cleavage complex is suboptimal for promoting transesterification to an exogenous 5′-OH oligonucleotide.

To better study cleavage and religation, we prepared oligonucleotide 30-mers containing *R* or *S* BPdA at position +1 or −2 of the nonscissile strand sequence $3'\text{-G}^{+5}\text{G}^{+4}\text{G}^{+3}\text{A}^{+2}\text{A}^{+1}\text{T}^{-1}\text{A}^{-2}$ and annealed them to a 5′-^{32}P-labeled 18-mer scissile strand to form 18-mer/30-mer suicide cleavage substrates for vaccinia TopIB (Figure 1). The cleavage transesterification reaction results in the covalent attachment of the ^{32}P-labeled 12-mer 5′-pCGTGTCGCCCTTp to the enzyme via Tyr274. The unlabeled 6-mer 5′-OH leaving strand dissociates spontaneously from the 12-mer-TopIB/30-mer complex. The loss of the leaving strand drives the reaction toward the covalent state so that the cleavage reaction can be treated kinetically as a first-order unidirectional process. The 18-mer 5′ tail on the cleavage complex suffices to recruit an exogenous complementary 5′-OH oligonucleotide for an analysis of single-turnover religation (*31*).

The cleavage reaction of excess TopIB with the unmodified control 18-mer/30-mer substrate attained an endpoint at which 94% of the DNA was converted to covalent

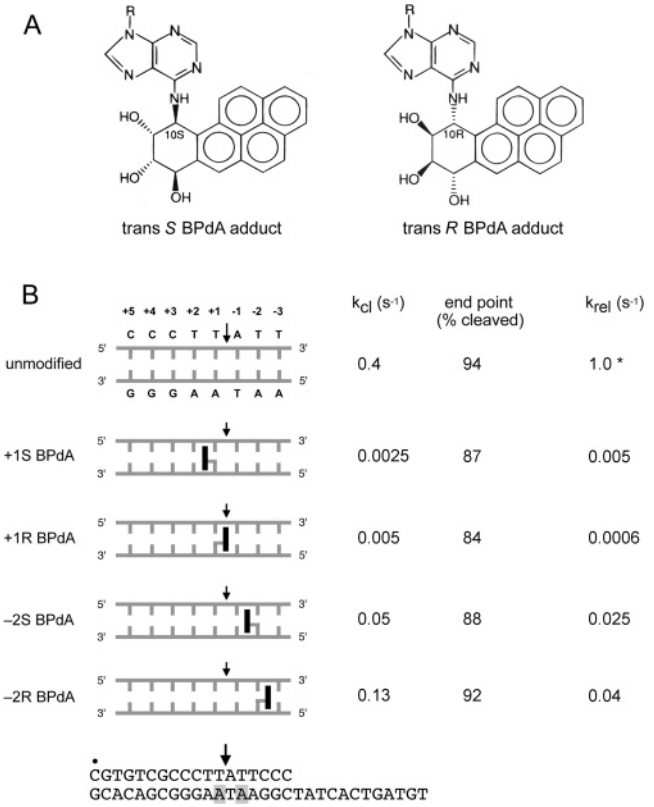

FIGURE 1: Effects of BPdA adducts on the rates of cleavage and religation by vaccinia TopIB. The chemical structures of the C-10 trans *S* and *R* BPdA adducts are shown (A), and the 18-mer/30-mer suicide substrate is at the bottom of the Figure with the site of cleavage indicated by a vertical arrow (B). The 5′-^{32}P label on the scissile strand is denoted by the dot. The unmodified control substrate is depicted in greater detail with the phosphodiester backbone drawn as horizontal lines and the base pairs as vertical lines. The numerical coordinates of the nucleotides are indicated above the control sequence. The *S* and *R* diastereomers of the BPdA adducts are depicted as intercalated vertical bars in their respective orientations on the 3′ side (*S*) or 5′ side (*R*) of the site of covalent attachment to adenine on the nonscissile strand. The rate constants and reaction endpoints for the forward cleavage reaction and the rate constants for single-turnover religation by the suicide intermediate are indicated to the right of each DNA substrate.

TopIB−DNA complex; the reaction was complete within 10 s. The extent of transesterification after 5 s was 88% of the endpoint value. From this datum, we calculated a single-turnover cleavage rate constant (k_{cl}) of 0.4 s^{-1} (Figure 1B). We found that the *S* and *R* BP modifications at position −2A slowed the cleavage rate on the 18-mer/30-mer to 0.13 and 0.05 s^{-1}, respectively, without significantly affecting the yield of covalently bound DNA at the reaction endpoint (Figure 1B and Figure 2A). These values agree with the rates reported previously for the suicide cleavage of the −2 BPdA-modified 34-mer/18-mer substrates (*12*). The slight stereoselective interference at −2A by the *S* diastereomer likely reflects the fact that the *S* adduct intercalates toward the scissile phosphodiester, whereas the *R* adduct is oriented away from the cleavage site. We found that the *S* and *R* BP adducts at +1A elicited cleavage rate decrements of 80-fold (k_{cl} = 0.0025 s^{-1}) and 160-fold (k_{cl} = 0.005 s^{-1}), respectively, without significantly affecting the endpoints (Figures 1B and 2A). The +1 BPdA effects on the cleavage of the 18-mer/30-mer were less severe (by factors of 6 to 8) than the rate

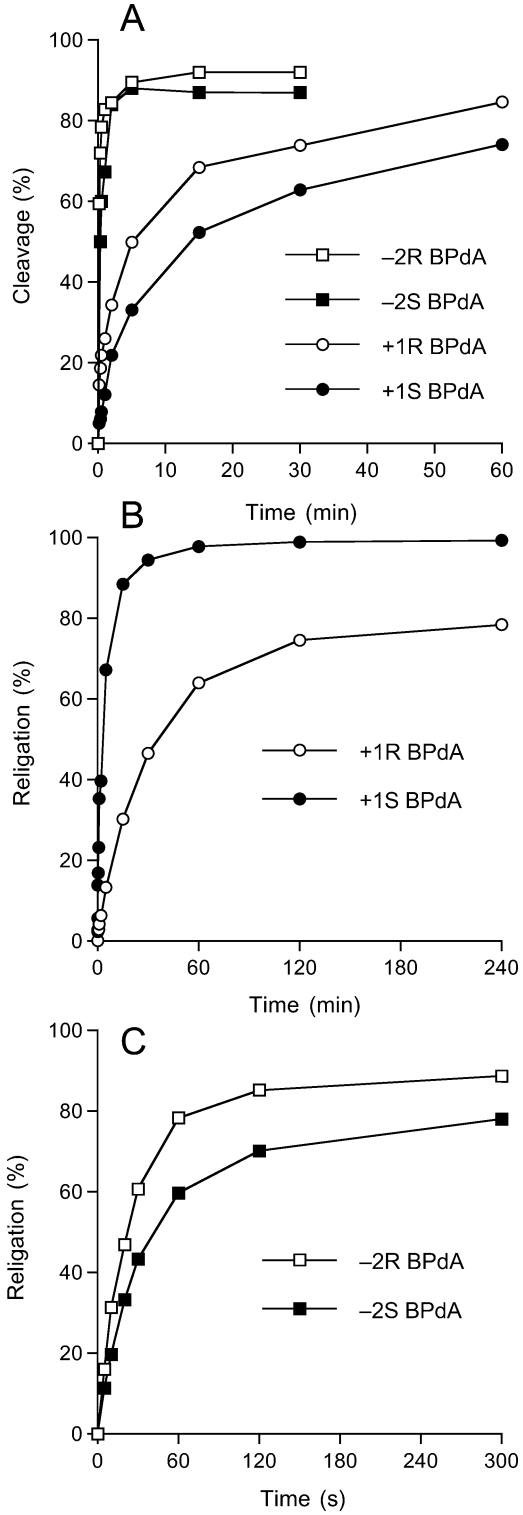

FIGURE 2: Kinetics of single-turnover cleavage and religation on BPdA-containing suicide substrates. Single-turnover cleavage (A) and religation (B and C) on 18-mer/30-mer substrates containing the indicated BPdA adducts were assayed as described under Experimental Procedures. The extents of the reactions are plotted as a function of time.

reductions reported previously for the cleavage of the 34-mer/18-mer substrates (*13*).

The religation step of the TopIB catalytic cycle entails the attack of the DNA 5′-OH on the covalent intermediate, leading to the expulsion of the Tyr274 leaving group and the restoration of the DNA phosphodiester backbone. The

effect of BPdA adducts on the religation reaction was studied under single-turnover conditions by assaying the ability of the preformed suicide intermediate to transfer the covalently held 5′-^{32}P-labeled 12-mer strand to a 5′ OH-terminated 18-mer strand to form a 30-mer product (*31*, *32*). After forming the suicide intermediate on the unmodified or adduct-containing 18-mer/30-mer substrates, the religation reaction was initiated by adding a 50-fold molar excess of the 18-mer 5′-OH DNA acceptor strand. The sequence of the added 18-mer is fully complementary to the 5′ single-stranded tail of the suicide intermediate. The ionic strength was adjusted simultaneously to 0.5 M NaCl to promote the dissociation of TopIB after strand ligation and prevent recleavage of the 30-mer strand transfer product. Aliquots were withdrawn immediately prior to the addition of the 18-mer and NaCl (defined as time 0) and at various times afterward, and the extent of religation at each time point was expressed as the fraction of the ^{32}P-labeled DNA present as covalent adduct at time zero that was converted to the 30-mer strand transfer product. The religation by TopIB bound covalently on unmodified DNA was complete within 5 s (not shown). The religation by the +1 *S*- and *R*-BPdA-modified covalent complexes was very slow (Figure 2B). The *S* and *R* reactions attained endpoints after 30 and 120 min, respectively, and the observed single-turnover religation rate constants (k_{rel}) of 0.005 and 0.0006 s^{-1} (Figure 1) were reduced by factors of 200 and 1700, respectively, compared to k_{rel} for the unmodified suicide intermediate (previously determined to be ~1.0 s^{-1}). The −2 BPdA adducts had more modest effects on the religation step (Figure 2C). The observed k_{rel} values of 0.025 and 0.04 s^{-1} for the −2 *S*- and *R*-BPdA complexes (Figure 1) were slowed by factors of 40 and 25. For each of the BPdA adducts, the effects on single-turnover religation rate was of greater magnitude than their effects on the single-turnover cleavage rate, which suggests that the PAH adducts might act as TopIB poisons.

BPdA Effects on the Cleavage−Religation Equilibrium of Vaccinia TopIB. A 5′-^{32}P-labeled CCCTT-containing 34-mer/30-mer containing 12 bp of DNA upstream of the cleavage site and 18 bp of DNA downstream of the cleavage site was employed to assay transesterification under equilibrium conditions (Figure 3). This DNA is an equilibrium substrate because the 5′-OH leaving strand generated upon cleavage at CCCTT remains stably associated with the TopIB−DNA complex via base pairing to the nonscissile strand. We determined by enzyme titration that vaccinia TopIB cleaved 22% of the unmodified substrate at saturation. The cleavage−religation equilibrium constant (K_{cl} = covalent complex/noncovalent complex = k_{cl}/k_{rel}) was thus 0.28 for the unmodified DNA.

The yield of the covalent intermediate as a function of input TopIB was determined for the four modified equilibrium substrates containing BPdA lesions at +1 and −2 in the nonscissile strand. All were cleaved to higher than control levels at saturating enzyme, with values ranging from 72 to 81% covalent adduct. The cleavage equilibrium constants were 4.1, 4.1, 2.6, and 3.4 for the +1*S*, +1*R*, −2*S* and −2*R* BPdA substrates, respectively (Figure 3). Thus, the +1 and −2 BPdA adducts exerted a significantly greater effect on religation than cleavage, as suggested by the single-turnover kinetic data obtained with the suicide substrates. Indeed, the experimental K_{eq} values of 2.6, 3.4, and 4.1 for the −2*S*, −2*R* and +1*R* BPdA equilibrium substrates (Figure 3) agreed reasonably well with the k_{cl}/k_{rel} values of 2.0, 3.25, and 8.3 calculated using the single-turnover rates on the 18-mer/30-mer (Figure 1). However, in the case of the +1*S* BPdA modification, the measured equilibrium constant (4.1) was much higher than the ratio of the single-turnover rates (0.5).

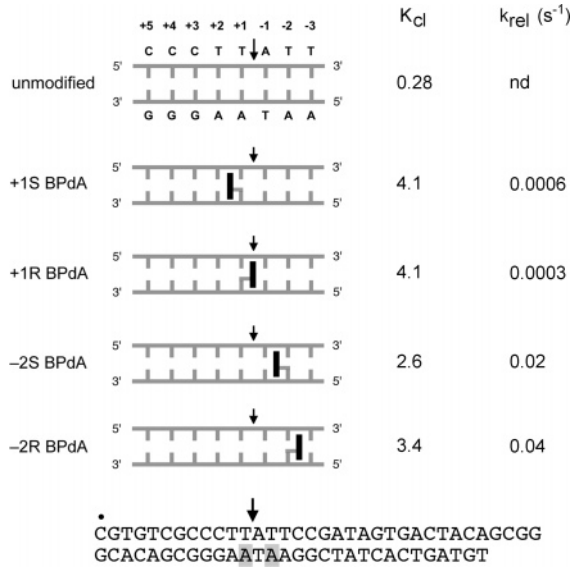

FIGURE 3: BPdA effects on the cleavage−religation equilibrium and single-turnover strand closure. The 34-mer/30-mer substrate is shown at the bottom of the figure with the site of cleavage indicated by a vertical arrow. The BPdA adducts at the +1A and −2A bases are shaded in gray. The unmodified and BPdA-containing substrates are depicted in greater detail as described in Figure 1. Equilibrium cleavage and single-turnover religation were assayed as described under Experimental Procedures. The experimental K_{cl} and k_{rel} values are indicated to the right of each DNA substrate.

The fact that the cleavage endpoints on the BPdA-modified equilibrium substrates were high facilitates an independent measurement of single-turnover religation by allowing the cleavage reaction to reach equilibrium on the 34-mer/30-mer and then adjusting the reaction mixtures to 0.5 M NaCl (*17*). This concentration of salt blocks DNA cleavage by interfering with DNA binding. TopIB pre-bound to an equilibrium cleavage substrate at low ionic strength is dissociated when the salt concentration is raised to 0.5 M. Hence, TopIB molecules that have catalyzed strand closure on the 34-mer/30-mer DNA will be dissociated from the DNA by salt and will be unable to rebind and recleave. The decrease in the covalent complex as a function of time after the addition of NaCl is plotted in Figure 4. The +1*S* and +1*R* BPdA covalent complexes declined slowly over 60 to 120 min (k_{rel} = 0.0006 s^{-1} and 0.0003 s^{-1} for the +1*S* and +1*R* BPdA DNAs, respectively) (Figures 3 and 4A). Note that the observed rate constant for single-turnover religation by the +1*R* BPdA-modified complex on the 34-mer/30-mer agreed (within a factor of 2) with the value measured for religation by the 12-mer/30-mer suicide intermediate. However, the rate of religation by the +1*S* BPdA complex on the 34-mer/30-mer was significantly slower (by a factor of 8) than that measured with the suicide intermediate. Yet, by using the equilibrium k_{rel} value and the suicide k_{cl} value, the resulting k_{cl}/k_{rel} ratio of 4.2 now agrees very well with the experimental K_{eq} value of 4.1 for the +1*S* BPdA-containing

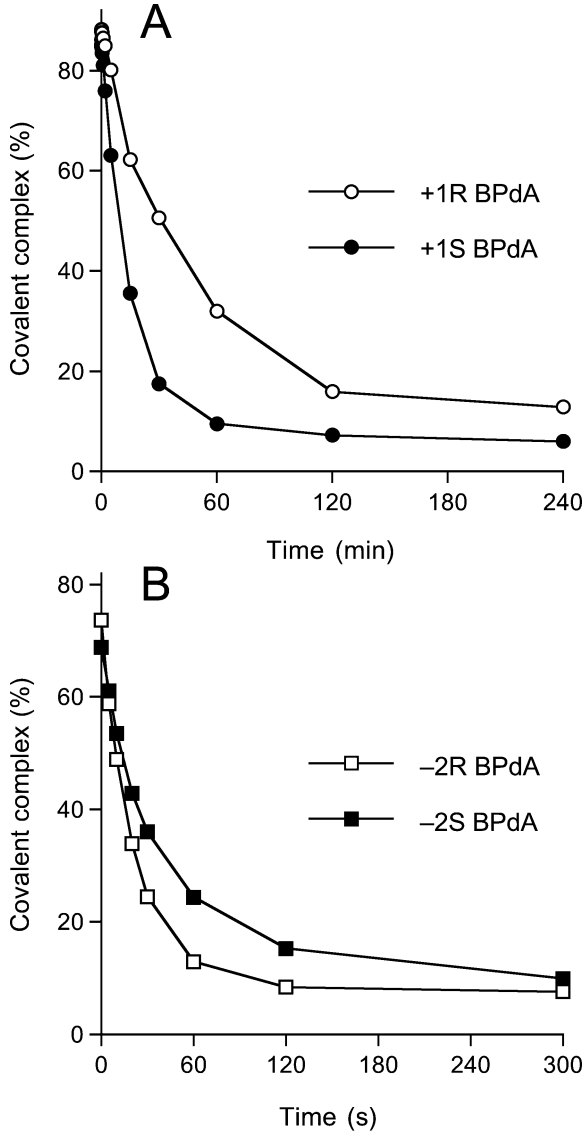

FIGURE 4: Kinetics of religation on the equilibrium substrate. Single-turnover religation by TopIB on the 34-mer/30-mer equilibrium substrates containing the *S* or *R* BPdA adducts at +1A (panel A) or −2A (panel B) was assayed as described in Experimental Procedures. The decay of the covalent intermediate is plotted as a function of time postaddition of 0.5 M NaCl.

substrate. From the rates of decline of the −2*S* and −2*R* BPdA covalent complexes in Figure 4B, we determined k_{rel} values of 0.02 and 0.04 s^{-1}, respectively (Figure 3), which are in good agreement with the religation rates measured with the suicide −2 BPdA-modified intermediates (Figure 1).

In summary, the single-turnover and equilibrium transesterification experiments show that intercalating BP adducts on either side of the scissile phosphodiester act as cleavage-trapping TopIB poisons, whether they exert modest (at position −2) or more severe (at position +1) effects on the rates of the individual transesterification steps. We did not test the effects of intercalating PAH adducts at the +2A, +3G, or +4G positions of the 3′-GGGAATA nonscissile strand sequence on religation because prior studies had shown that those adducts strongly suppress (and in some instances abolish) the yield of the covalent TopIB−DNA intermediate (*13*, *14*).

Effects of Intercalating PAH Adducts on Exonuclease III. *E. coli* ExoIII catalyzes unidirectional digestion of duplex DNA from the 3′ end to liberate 5′ dNMP products. The phosphodiesterase activity of exonuclease III is impeded by various chemical modifications of the phosphate backbone (*33*−*35*) and by nonintercalating BPdG adducts that fit into the minor groove (*12*). Here, we tested the effects on ExoIII of intercalating BPdA adducts. The 5′-^{32}P-labeled 18-mers containing the unmodified or +1 or +2 BPdA-modified complements of the TopIB cleavage site were annealed to an unlabeled 34-mer strand to form the substrates shown in Figure 5. These DNAs were incubated for 1, 10, or 30 min with ExoIII, and the 5′-labeled digestion products were resolved by denaturing gel electrophoresis (Figure 5). Most of the unmodified control 18-mer was converted after 1 min to a cluster of 5′-labeled species 3 to 5 nucleotides in length. A faint ladder of partially digested strands was evident at 1 min and declined at later times. Initial digestion of the BP-modified DNAs by ExoIII was unaffected, as gauged by the rate of decay of the full-length 18-mer strand, but the nuclease was apparently arrested midway through the modified strands (Figure 5). Note that although the electrophoretic mobility of the BPdA-containing strands was retarded compared to the unmodified control strand, we were able to assign the 3′ ends of the digestion products using the partial digest ladder of each substrate seen at the 1 min time points.

The *R* and *S* BPdA adducts at +1A impeded ExoIII digestion after 1 min at sites 3 to 4 nucleotides 3′ of the lesions. The enzyme progressed by 10 min to positions 1 and 2 nucleotides 3′ of the +1*R* adduct site and 1, 2, and 3 nucleotides preceding the +1*S* adduct site but essentially went no further after 30 min, at which time there was only a trace of fully digested product detected at the bottom of the gel (Figure 5A). We surmise that BPdA adducts are durable roadblocks to ExoIII, which are practically unresectable by the nuclease. A similar kinetic pattern of durable 30-min arrest was seen with the +2*R* and +2*S* BPdA substrates, except that the arrest sites were phased by 1 nucleotide in the 3′ direction (Figure 5B). ExoIII was blocked 1 and 2 nucleotides away from the +2*R* BPdA adduct and 2 nucleotides away from the +2*S* BPdA adduct after 30 min of digestion.

In the experiments shown in Figure 5, we also probed the effects of benzo[*c*]phenanthrene (BPh) dA adducts at the +1 and +2 positions within the same substrate DNAs. BPh exemplifies the sterically hindered, nonplanar fjord-region class of PAHs. Activated BPh diol epoxides react at the benzylic C1 position by the trans addition of adenine N^6 in DNA to form covalent *S* and *R* BPhdA adducts. The BPh intercalates from the major groove such that the hydrocarbon portion of the *S* diastereomer is on the 3′ side of the modified dA base and that of the *R* diastereomer on the 5′ side (*36*, *37*). We found that ExoIII digestion of the +1*R* BPhdA substrate was arrested after 1 min at sites 2 and 3 nucleotides upstream of the modified base. ExoIII advanced to positions 1 and 2 nucleotides away from the adduct after 10 min (Figure 5A). Note that a significant fraction of the BPh-containing substrate was degraded to completion after 10 min, and nearly all of the BPh-containing strand was fully digested after 30 min. Thus, the *R* BPhdA adduct elicited a transient arrest of ExoIII that was overcome as the adducted nucleotide was resected from the DNA substrate. The *S* BPh

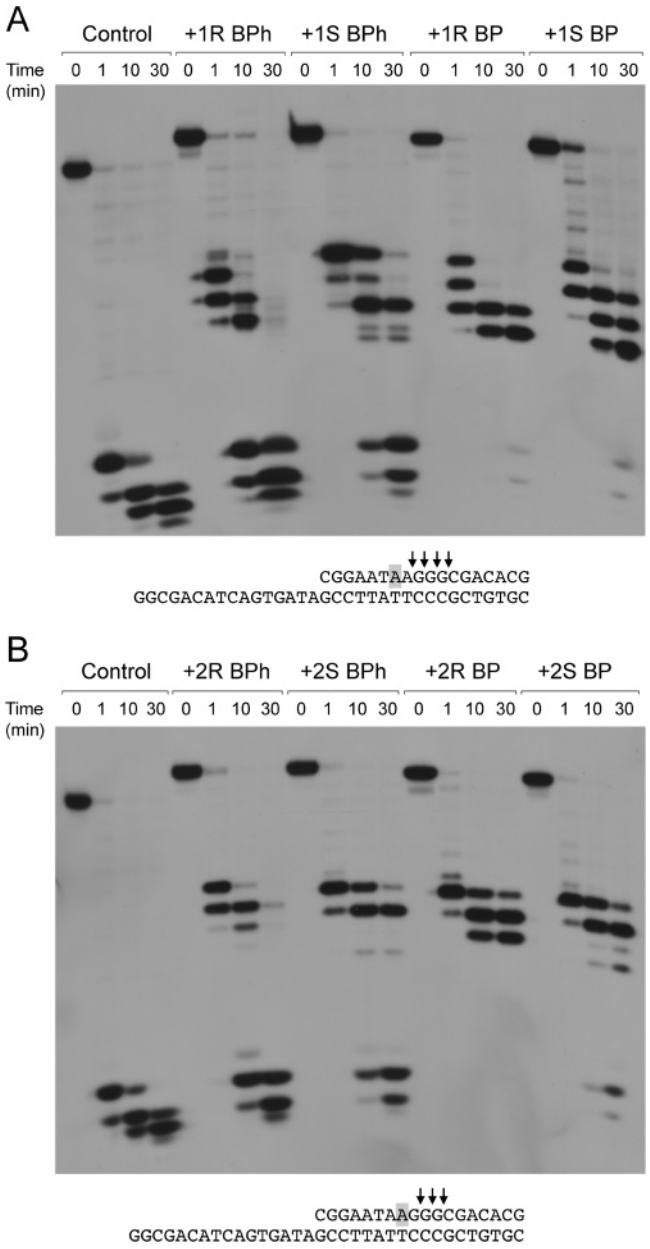

FIGURE 5: Effects of BPdA and BPhdA adducts on ExoIII. The 5′-^{32}P-labeled control and BPdA- or BPhdA-containing 18-mer oligonucleotides were annealed to a 34-mer to form the tailed duplex molecules shown below the autoradiograms. The BPdA adduct is shaded in gray. In panel A the adducts are at position +1 and in panel B, at position +2 (the numbering follows the TopIB nomenclature in Figure 1A). The DNAs were digested with ExoIII for 0, 1, 10, or 30 min. The products were analyzed by PAGE. The major ExoIII pause/arrest sites induced by the adducts are indicated by arrows over the sequences of the PAH-modified strands.

modification at +1A caused pausing after 1 min at a site 4 nucleotides away from the lesion (Figure 5A). ExoIII moved forward to within 2 nucleotides of the +1*S* BPhdA adduct by 10 min and then traversed the adduct between 10 and 30 min to yield a mixture of arrested and fully digested products (Figure 5A). Similar transient arrests were seen during ExoIII digestion of the +2*R* and +2*S* BPhdA-containing substrates (Figure 5B). These experiments reveal a difference in the ability of a repair nuclease to excise BPhdA versus BPdA adducts from duplex DNA.

We also probed the effects of position-specific intercalation by BcPh adducts at guanosine (dG) nucleosides within the 3′-$G^{+5}G^{+4}G^{+3}A^{+2}A^{+1}T^{-1}A^{-2}$ sequence of the 18-mer strand. In these cases, the PAH ring is attached to guanine N^2 (Figure 6A) and intercalated via the minor groove. The *S* diastereomer intercalates on the 5′ side of the dG, whereas the *R* diastereomer intercalates on the 3′ side (*38*). In the case of the +3*R* and +3*S* BPhdG-modified substrates, exonuclease III was sharply arrested after removing 6 nucleotides; digestion of the +4*R* and +4*S* BPhdG substrates was halted after the excision of 5 nucleotides; the +5*R* and +5*S* BPhdG substrates were shortened by 4 nucleotides (Figure 6B). The sites of ExoIII arrest were situated 3 nucleotides upstream of the lesions, and the arrests were durable over the 30 min incubations such that virtually no excision past the BPhdG adducts was detected (Figure 6B). These results for BPhdG contrast with the ability of ExoIII to excise BPhdA lesions, and they underscore the themes that (i) ExoIII closely surveys the minor groove ahead of the active site of catalysis and (ii) the same PAH ring can exert distinct effects on DNA repair depending on its route of intercalation via the major or minor groove.

DISCUSSION

The mutagenic effects of PAH−DNA adducts are well-known, but analyses of their impact on individual enzymes of nucleic acid metabolism is a relatively young field. Many studies have focused on how PAH lesions are handled by DNA polymerases and how the adducts affect the cleavage−religation cycle of DNA topoisomerases. With respect to DNA polymerases, PAH adducts in the template strand can either arrest replication fork progression or promote nucleotide misincorporation, either of which can result in mutations. PAH adducts can affect topoisomerases either by inhibiting the DNA binding and forward cleavage steps that generate the covalent enzyme−DNA intermediate or by slowing the DNA religation step or both. The outcome of the encounter of a topoisomerase with a PAH adduct depends on the position of the adduct relative to that of the scissile phosphodiester, the chemical structure of the adduct, whether it intercalates or occupies the minor groove, and its stereochemical configuration. The consequences of inhibiting the religation step of the topoisomerase reaction are, in principle, much greater than the inference with cleavage, insofar as the covalently trapped intermediates are themselves toxic lesions that promote genome instability if not rectified.

The studies here of intercalating BPdA adducts on the religation reaction kinetics and the cleavage equilibrium of vaccinia TopIB extend and complement earlier studies of PAH effects on the extent and rate of DNA cleavage by human and vaccinia TopIB, respectively (*7*−*9*, *12*−*14*). The key findings here are that BPdA adducts at positions +1 and −2 that flank the cleavage site act as TopIB poisons. BP adducts at +1A within the vaccinia TopIB target sequence elicit greater effects on the rates of cleavage and religation than do the relatively well-tolerated lesions at position −2A. Yet, the +1 BPdA adducts are actually better poisons because the K_{eq} values on the +1 BPdA substrates are higher than those measured on the −2 BPdA-containing DNAs.

A simple interpretation of the data is that intercalating BPdA adducts inhibit transesterification as a consequence

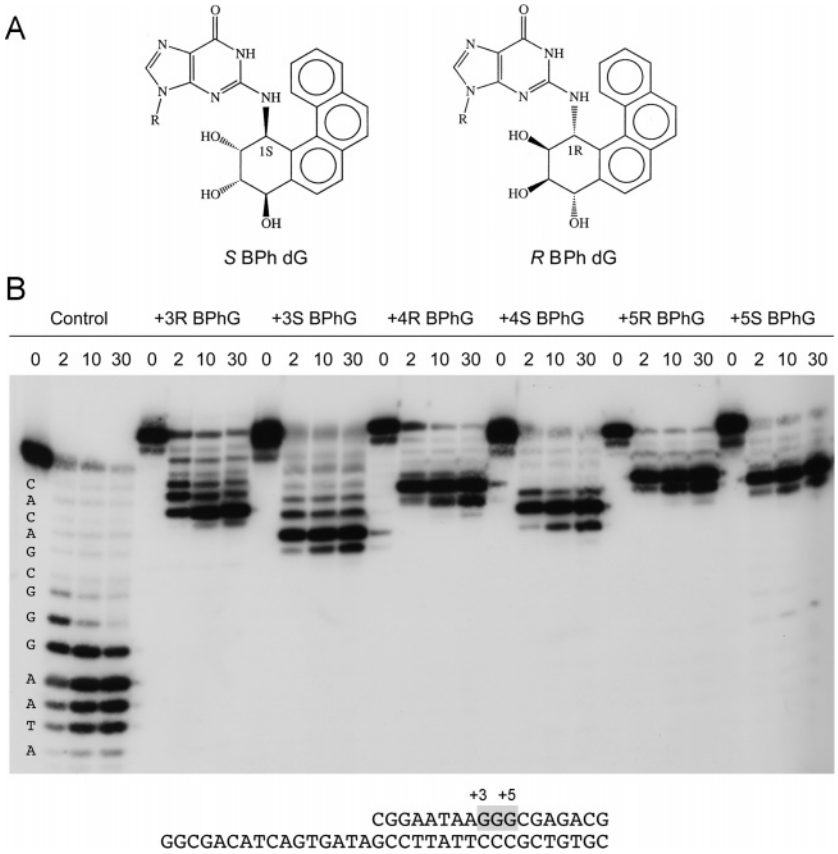

FIGURE 6: Effect of BPhdG adducts on ExoIII. (A) Chemical structures of the C-1 trans opened *S* and *R* BPhdG adducts. (B) The 5′-^{32}P-labeled control and BPhdG-containing 18-mer oligonucleotides were annealed to a 34-mer to form the tailed duplex molecule shown below the autoradiogram. The BPhdG-modified bases are shaded in gray. The DNAs were digested with ExoIII for 0, 2, 10, or 30 min. The products were analyzed by PAGE. The nucleotide sequence of the 18-mers is displayed next to the cleavage ladder of the unmodified strand, with each letter specifying the 3′ nucleotide of the indicated radiolabeled species. The 3′ termini of the ExoIII-digested BPhdG-adducted oligonucleotides, which migrated slower than the unmodified strands of identical length, could be deduced from the single-nucleotide spacing of the oligonucleotide ladders. Note that the oligonucleotides containing *S* BPhdG adducts migrated faster than the corresponding *R* BPhdG-adducted oligonucleotides.

of disruption or weakening of important contacts between TopIB and either the bases or backbone phosphates of the DNA target site (*39*−*41*). What is not clear is why these perturbations would have a quantitatively greater impact on religation than on cleavage. This outcome implies that at least some DNA−protein contacts differ in their importance during the forward and reverse transesterification steps or that the atomic contacts are remodeled during the catalytic cycle. Previous studies have shown that certain missense mutations in vaccinia TopIB result in an increase in the equilibrium constant (*17*, *31*, *32*). Even more pertinent to the present study is the report that abasic lesions at positions +1 and −1 on the nonscissile strand can act as highly potent poisons of vaccinia TopIB, increasing the equilibrium constant to values of 11.5 and 15.7, respectively, and slowing the rates of single-turnover religation to 0.0072 and 0.044 s^{-1}, respectively (*40*). The similar poisoning effects of intercalating PAH adducts and abasic lesions in the nonscissile strand flanking the cleavage site hint that these structurally distinct lesions might perturb the same contact within the covalent TopIB−DNA intermediate.

The observation that the religation rate in the presence of a +1*S* BPdA lesion is slower when the equilibrium cleavage complex already contains the acceptor oligonucleotide (0.0006 s^{-1}) than when the acceptor is introduced exogenously into a 5′-tailed suicide complex (0.005 s^{-1}) suggests that the equilibrium and suicide covalent complexes differ in conformation. A possible interpretation is that upon cleavage of the equilibrium substrate the bulky hydrocarbon adduct immediately assumes a conformation that interferes with the proper orientation of the 5′-hydroxyl nucleophile at residue −1 and thus severely impedes religation. An analogous mechanism has been proposed for the poisoning of human Top1B by a +1*R* BPdA adduct in the nonscissile strand (*8*). The suicide intermediate, which contains a 5′ single stranded tail, might be more flexible and adopt a different conformation in which the hydrocarbon exerts less interference on the reaction with an incoming oligonucleotide.

The mutagenic impact of different PAH adducts entails a balance between their ability to induce mutations (via enzymes such as polymerases and topoisomerases) and the ability of repair enzymes to eliminate the adducts from DNA before they cause lasting genetic changes. There is evidence that PAH adducts are recognized by the nucleotide excision repair (NER) system, although recognition does not necessarily mean a capacity to repair the lesion efficiently (*20*−*22*). For example, it was reported that a BPhdA adduct was refractory to repair in human cell extracts, whereas a BPdA adduct at the same site in the synthetic DNA substrate was removed (*21*). Here, we analyzed the ability of a DNA repair nuclease, *E. coli* ExoIII, to excise intercalating BPdA and

BPhdA adducts from a duplex DNA substrate. We find that BPhdA adducts can be excised by ExoIII, albeit slowly, whereas BPdA adducts in the same positions are refractory to digestion and cause a durable arrest to the progression of ExoIII at discrete sites prior to the adducted nucleotide. The repair fates of BPhdA versus BPdA were inverted in our ExoIII experiments compared to what had been observed for NER in cell extracts (*21*), which underscores the theme that different pathways or individual repair enzymes will handle PAH adducts in distinctive ways. Indeed, we see that the fjord-type BPh ring system has a more severe effect on ExoIII when intercalated via the minor groove at dG positions versus when intercalated at dA through the major groove. These results highlight repair nucleases as worthy subjects for a more comprehensive survey of PAH adduct effects. They also recommend PAH adduct interference as a method to delineate the functional interface between a repair enzyme and DNA.

ACKNOWLEDGMENT

S.S. is an American Cancer Society Research Professor.

REFERENCES

1. Thakker, D. R., Yagi, H., Levin, W., Wood, A. W., Conney, A. H. and Jerina, D. M. (1985) Polycyclic aromatic hydrocarbons: Metabolic activation to ultimate carcinogens. In *Bioactivation of Foreign Compounds* (Anders, M. W., Ed.) pp 177−242, Academic Press, New York.
2. Jerina, D. M., Chadha, A., Cheh, A. M., Schurdak, M. E., Wood, A. W., and Sayer, J. M. (1991) Covalent bonding of bay-region diol epoxides to nucleic acids. In *Biological Reactive Intermediates IV. Molecular and Cellular Effects and Their Impact on Human Health* (Witmer, C. M., Snyder, R., Jollow, D. J., Kalf, G. F., Kocsis, J. J., Sipes, I. G., Eds.) pp 533−553, Plenum Press, New York.
3. Geacintov, N. E., Cosman, M., Hingerty, B. E., Amin, S., Broyde, S., and Patel, D. J. (1997) NMR structures of stereoisomeric covalent polycyclic aromatic carcinogen-DNA adducts: principles, patterns, and diversity, *Chem. Res. Toxicol. 10*, 111−146.
4. Chiapperino, D., Cai, M., Sayer, J. M., Yagi, H., Kroth, H., Masutani, C., Hanaoka, F., Jerina, D. M., and Cheh A. M. (2005) Error-prone translesion synthesis by human DNA polymerase on DNA containing deoxyadenosine adducts of 7,8-dihydroxy-9,10-epoxy-7,8,9,10-tetrahydrobenzo[*a*]pyrene, *J. Biol. Chem. 280*, 39684−39692.
5. Ling, H., Sayer, J. M., Plosky, B. S., Yagi, H., Boudsocq, F., Woodgate, R., Jerina, D. M., and Yang, W. (2004) Crystal structure of a benzo[*a*]pyrene diol epoxide adduct in a ternary complex with a DNA polymerase, *Proc. Natl. Acad. Sci. U.S.A. 101*, 2265−2269.
6. Hsu, G. W., Huang, X., Luneva, N. P., Geacintov, N. E., and Beese, L. S. (2005) Structure of a high fidelity DNA polymerase bound to a benzo[*a*]pyrene adduct that blocks DNA replication, *J. Biol. Chem. 280*, 3764−3770.
7. Pommier, Y., Kohlhagen, G., Pourquier, P., Sayer, J. M., Kroth, H., and Jerina, D. M. (2000) Benzo[*a*]pyrene diol epoxide adducts in DNA are potent suppressors of a normal topoisomerase I cleavage site and powerful inducers of other topoisomerase I cleavages, *Proc. Natl. Acad. Sci. U.S.A. 97*, 2040−2045.
8. Pommier, Y., Laco, G. S., Kohlhagen, G., Sayer, J. M., Kroth, H., and Jerina, D. M. (2000) Position-specific trapping of topoisomerase I-DNA cleavage complexes by intercalated benzo-[*a*]pyrene diol epoxide adducts at the 6-amino group of adenine, *Proc. Natl. Acad. Sci. U.S.A. 97*, 10739−10744.
9. Pommier, Y., Kohlhagen, G., Laco, G. S., Kroth, H., Sayer, J. M., and Jerina, D. M. (2002) Differential effects on human topoisomerase I by minor groove and intercalated deoxyguanine adducts derived from two polycyclic aromatic hydrocarbon diol epoxides at or near a normal cleavage site, *J. Biol. Chem. 277*, 13666−13672.
10. Khan, Q. A., Kohlhagen, G., Marshall, R., Austin, C. A., Kalena, G. P., Kroth, H., Sayer, J. M., Jerina, D. M., and Pommier, Y. (2003) Position-specific trapping of topoisomerase II by benzo-[*a*]pyrene diol epoxide adducts: implications for interactions with intercalating anticancer agents, *Proc. Natl. Acad. Sci. U.S.A. 100*, 12498−12503.
11. Hsiang, Y. H., Hertzberg, R., Hecht, S., and Liu, L. F. (1985) Camptothecin induces protein-linked DNA breaks via mammalian DNA topoisomerase I, *J. Biol. Chem. 260*, 14873−14878.
12. Tian, L., Sayer, J. M., Kroth, H., Kalena, G., Jerina, D. M., and Shuman, S. (2003) Benzo[*a*]pyrene-dG adduct interference illuminates the interface of vaccinia topoisomerase with the DNA minor groove, *J. Biol. Chem. 278*, 9905−9911.
13. Yakovleva, L., Tian, L., Sayer, J. M., Kalena, G. P., Kroth, H., Jerina, D. M., and Shuman, S. (2003) Site-specific DNA transesterification by vaccinia topoisomerase: effects of benzo[*a*]-pyrene-dA, 8-oxoguanine, 8-oxoadenine and 2-aminopurine modifications, *J. Biol. Chem. 278*, 42170−42177.
14. Yakovleva, L., Handy, C. J., Sayer, J. M., Pirrung, M., Jerina, D. M., and Shuman, S. (2004) Benzo[*c*]phenanthrene adducts and nogalamycin inhibit DNA transesterification by vaccinia topoisomerase, *J. Biol. Chem. 279*, 23335−23342.
15. Shuman, S., and Prescott, J. (1990) Specific DNA cleavage and binding by vaccinia virus DNA topoisomerase I, *J. Biol. Chem. 265*, 17826−17836.
16. Stivers, J. T., Shuman, S., and Mildvan, A. S. (1994) Vaccinia DNA topoisomerase I: single-turnover and steady-state kinetic analysis of the DNA strand cleavage and ligation reactions, *Biochemistry 33*, 327−339.
17. Wittschieben, J., and Shuman, S. (1997) Mechanism of DNA transesterification by vaccinia topoisomerase: catalytic contributions of essential residues Arg-130, Gly-132, Tyr-136, and Lys-167, *Nucleic Acids Res. 25*, 3001−3008.
18. Stivers, J. T., Jagadeesh, G. J., Nawrot, B., Stec, W. J., and Shuman, S. (2000) Stereochemical outcome and kinetic effects of *R*p and *S*p phosphorothioate substitutions at the cleavage site of vaccinia type I DNA topoisomerase, *Biochemistry 39*, 5561−5572.
19. Hess, M. T., Gunz, D., Luneva, N., Geacintov, N. E., and Naegeli, H. (1997) Base pair conformation-dependent excision of benzo-[*a*]pyrene diol epoxide-guanine adducts by human excision repair enzymes, *Mol. Cell. Biol. 17*, 7069−7076.
20. Buterin, T., Hess, M. T., Luneva, N., Geacintov, N. E., Amin, S., Kroth, H., Seidel, A., and Naegeli, H. (2000) Unrepaired fjord region polycyclic aromatic hydrocarbon-DNA adducts in ras codon 61 mutation hot spots, *Cancer Res. 60*, 1849−1856.
21. Buterin, T., Hess, M. T., Gunz, D., Geacintov, N. E., Mullenders, L. H., and Naegeli, H. (2002) Trapping of DNA nucleotide excision repair factors by nonrepairable carcinogen adducts, *Cancer Res. 62*, 4229−4235.
22. Mol, C. D., Kuo, C. F., Thayer, M. M., Cunningham, R. P., and Tainer, J. A. (1995) Structure and function of the multifunctional DNA-repair enzyme exonuclease III, *Nature 374*, 381−386.
23. Gorman, M. A., Morera, S., Rothwell, D. G., de La Fortelle, E., Mol, C. D., Tainer, J. A., Hickson, I. D., and Freemont, P. S. (1997) The crystal structure of the human DNA repair endonuclease HAP1 suggest the recognition of extra-helical deoxyribose at DNA abasic sites, *EMBO J. 16*, 6548−6558.
24. Weston, S. S., Lahm, A., and Suck, D. (1992) X-ray structure of the DNase I-d(GGTATACC)2 complex at 2.3 Å resolution, *J. Mol. Biol. 226*, 1237−1265.
25. Kroth, H., Yagi, H., Sayer, J. M., Kumar, S., and Jerina, D. M. (2001) O^6-Allyl protected deoxyguanosine adducts of polycyclic aromatic hydrocarbons as building blocks for the synthesis of oligonucleotides, *Chem. Res. Toxicol. 14*, 708−719.
26. Volk, D. E., Rice, J. S., Luxon, B. A., Yeh, H. J. C., Liang, C., Xie, G., Sayer, J. M., Jerina, D. M., and Gorenstein, D. G. (2000) NMR evidence for syn-anti interconversion of a trans opened (10*R*)-dA adduct of benzo[*a*]pyrene (7*S*,8*R*)-diol (9*R*,10*S*)-epoxide in a DNA duplex, *Biochemistry 39*, 14040−14053.
27. Pradhan, P., Tirumala, S., Liu, X., Sayer, J. M., Jerina, D. M., and Yeh, H. J. C. (2001) Solution structure of a trans-opened (10*S*)-dA adduct of (+)-(7*S*,8*R*,9*S*,10*R*)-7,8-dihydroxy-9,10-epoxy-7,8,9,10-tetrahydrobenzo[*a*]pyrene in a fully complementary DNA duplex: Evidence for a major syn conformation, *Biochemistry 40*, 5870−5881.
28. Zegar, I. S., Chary, P., Jabil, R. J., Tamura, P. J., Johansen, T. N., Lloyd, R. S., Harris, C. M., Harris, T. M., and Stone, M. P. (1998)

Multiple conformations of an intercalated (−)-(7*S*,8*R*,9*S*,10*R*)-N^6-[10-(7,8,9,10-tetrahydrobenzo[*a*]pyrenyl)]-2′-deoxyadenosyl adduct in the *N-ras* codon 61 sequence, *Biochemistry 37*, 16516−16528.

29. Schurter, E. J., Sayer, J. M., Oh-hara, T., Yeh, H. J. C., Yagi, H., Luxon, B. A., Jerina, D. M., and Gorenstein, D. G. (1995) Nuclear magnetic resonance solution structure of an undecanucleotide duplex with a complementary thymidine base opposite a 10*R* adduct derived from trans addition of a deoxyadenosine N^6-amino group to (−)-(7*R*,8*S*,9*R*,10*S*)-7,8-dihydroxy-9,-10-epoxy-7,8,9,10-tetrahydrobenzo[*a*]pyrene, *Biochemistry 34*, 9009−9020.
30. Zegar, I. S., Kim, S. J., Johansen, T. N., Horton, P. J., Harris, C. M., Harris, T. M., and Stone, M. P. (1996) Adduction of the human *N-ras* codon 61 sequence with (−)-(7*S*,8*R*,9*R*,10*S*)-7,8-dihydroxy-9,10-epoxy-7,8,9,10-tetrahydrobenzo[*a*]pyrene: Structural refinement of the intercalated SRSR(61,2) (−)-(7*S*,8*R*,9*S*,-10*R*)-N^6-[10-(7,8,9,10-tetrahydro-benzo[*a*]pyrenyl)]-2′-deoxyadenosyl adduct from ^{1}H NMR, *Biochemistry 35*, 6212−6224.
31. Petersen, B. Ø., and Shuman, S. (1997) Histidine-265 is important for covalent catalysis by vaccinia topoisomerase and is conserved in all eukaryotic type I enzymes, *J. Biol. Chem. 272*, 3891−3896.
32. Cheng, C., Wang, L. K., Sekiguchi, J., and Shuman, S. (1997) Mutational analysis of 39 residues of vaccinia DNA topoisomerase identifies Lys-220, Arg-223, and Asn-228 as important for covalent catalysis, *J. Biol. Chem. 272*, 8263−8269.
33. Krogh, B. O., Claeboe, C. D., Hecht, S. M., and Shuman, S. (2001) Effect of 2′-5′ phosphodiesters on DNA transesterification by vaccinia topoisomerase, *J. Biol. Chem. 276*, 20907−20912.
34. Putney, S. D., Benkovic, S. J., and Schimmel, P. R. (1981) A DNA fragment with an α-phosphorothioate nucleotide at one end is asymmetrically blocked from digestion by exonuclease III and can be replicated *in vivo*, *Proc. Natl. Acad. Sci. U.S.A. 78*, 7350−7354.
35. Porter, K. W., Briley, J. D., and Shaw, B. R. (1997) Direct PCR sequencing with boronated nucleotides, *Nucleic Acids Res. 25*, 1611−1617.
36. Cosman, M., Fiala, R., Hingerty, B. E., Laryea, A., Lee, H., Harvey, R. G., Amin, S., Geacintov, N. E., Broyde, S., and Patel, D. J. (1993) Solution conformation of the (+)-trans-anti-[BPh]-dA adduct opposite dT in a DNA duplex: Intercalation of the covalently attached benzo[*c*]phenanthrene to the 5′-side of the adduct site without disruption of the modified base pair, *Biochemistry 32*, 12488−12497.
37. Cosman, M., Laryea, A., Fiala, R., Hingerty, B. E., Amin, S., Geacintov, N. E., Broyde, S., and Patel, D. J. (1995) Solution conformation of the (−)-trans-anti-benzo[*c*]phenanthrene-dA ([BPh]-dA) adduct opposite dT in a DNA duplex: intercalation of the covalently attached benzo[*c*]phenanthrenyl ring to the 3′-side of the adduct site and comparison with the (+)-trans-anti-[BPh]dA opposite dT stereoisomer, *Biochemistry 34*, 1295−1307.
38. Lin, C. H., Huang, X., Kolbanovskii, A., Hingerty, B. E., Amin, S., Broyde, S. Geacintov, N. E., and Patel, D. J. (2001) Molecular topology of polycyclic aromatic carcinogens determines DNA adduct conformation: a link to tumorigenic activity, *J. Mol. Biol. 306*, 1059−1080.
39. Tian, L., Claeboe, C. D., Hecht, S. M., and Shuman, S. (2004) Remote phosphate contacts trigger assembly of the active site of DNA topoisomerase IB, *Structure 12*, 31−40.
40. Tian, L., Sayer, J. M., Jerina, D. M., and Shuman, S. (2004) Individual nucleotide bases, not base pairs, are critical for triggering site-specific DNA cleavage by vaccinia topoisomerase, *J. Biol. Chem. 279*, 39718−39726.
41. Tian, L., Claeboe, C. D., Hecht, S. M., and Shuman, S. (2005) Mechanistic plasticity of DNA topoisomerase IB: phosphate electrostatics dictate the need for a catalytic arginine, *Structure 13*, 513−520.

BI060158H